AIAA 2003-4198

Thermal Contact Resistance of Non-Conforming Rough Surfaces, Part 2: Thermal Model

M. Bahrami, J. R. Culham, M. M. Yovanovich and G. E. Schneider
Microelectronics Heat Transfer Laboratory
Department of Mechanical Engineering
University of Waterloo, Waterloo
Ontario, Canada N2L 3G1

36th AIAA Thermophysics Conference
Meeting and Exhibit
June 23-26, 2003/Orlando, Florida

Thermal Contact Resistance of Non-Conforming Rough Surfaces, Part 2: Thermal Model

M. Bahrami*, J. R. Culham†, M. M. Yovanovich‡ and G. E. Schneider§
Microelectronics Heat Transfer Laboratory
Department of Mechanical Engineering
University of Waterloo, Waterloo
Ontario, Canada N2L 3G1

Thermal contact resistance (TCR) of non-conforming rough surfaces is studied and a new analytical model is developed. TCR is considered as the superposition of macro and micro components accounting for the effects of surface curvature and roughness, respectively. The effects of roughness, load and radius of curvature on TCR are investigated. It is shown that there is a value of surface roughness that minimizes the TCR. Simple correlations for determining TCR, using the general pressure distribution introduced in Part 1 of this study, are derived which cover the entire range of TCR ranging from conforming rough to smooth spherical contacts. The comparison of the present model with more than 700 experimental data points shows good agreement in the entire range of TCR.

Nomenclature

A	=	area, (m^2)
a	=	radius of contact, (m)
b	=	flux tube radius, (m)
a'_L	=	relative radius of macrocontact, a_L/a_{Hz}
b_L	=	specimens radius, (mm)
B	=	relative macrocontact radius, a_L/b_L
CS	=	Carbon Steel
c_1	=	Vickers microhardness coefficient, (GPa)
c_2	=	Vickers microhardness coefficient, $(-)$
d_v	=	Vickers indentation diagonal, (μm)
dr	=	increment in radial direction, (m)
E'	=	equivalent elastic modulus, (GPa)
F	=	external force, (N)
h	=	contact conductance, $\left(W/m^2K\right)$
H_{mic}	=	microhardness, (GPa)
H'	=	$c_1\left(1.62\sigma'/m\right)^{c_2}$, (GPa)
k	=	thermal conductivity, (W/mK)
m	=	mean absolute surface slope, $(-)$
n_s	=	number of microcontacts
P	=	pressure, (Pa)
P'_0	=	relative maximum pressure, $P_0/P_{0,Hz}$
Q	=	heat flow rate, (W)
R	=	thermal resistance, (K/W)
r, z	=	cylindrical coordinates
s	=	$0.95/\left(1+0.071c_2\right)$
Y	=	mean surface plane separation, (m)

Greek

α	=	non-dimensional parameter, $\sigma\rho/a^2_{Hz}$
γ	=	general pressure distribution exponent
δ	=	maximum surface out-of-flatness, (m)
ε	=	flux tube relative radius, a_s/b_s
η_s	=	microcontacts density, $\left(m^{-2}\right)$
κ	=	$H_B/\ H_{BGM}$
λ	=	dimensonless separation, $Y/\sqrt{2}\sigma$
ξ	=	dimensionless radial position, r/a_L
ψ	=	spreading resistance factor
ρ	=	radius of curvature, (m)
σ	=	RMS surface roughness, (μm)
τ	=	non-dimensional parameter, ρ/a_{Hz}
Ω	=	dimensionless parameter

Subscripts

0	=	value at origin
$1,2$	=	solid 1, 2
a	=	apparent
B	=	Brinell
b	=	bulk
c	=	critical
Hz	=	Hertz
j	=	joint
L	=	macro
mac	=	macro
mic	=	micro
r	=	real
s	=	macro, solid
v	=	Vickers

Introduction

Heat transfer across interfaces formed by mechanical contact of two non-conforming rough solids occurs in a wide range of applications, such as: microelec-

*Ph.D. Candidate, Department of Mechanical Engineering.
†Associate Professor, Director, Microelectronics Heat Transfer Laboratory.
‡Distinguished Professor Emeritus, Department of Mechanical Engineering. Fellow AIAA.
§Professor, Department of Mechanical Engineering. Associate Fellow AIAA.

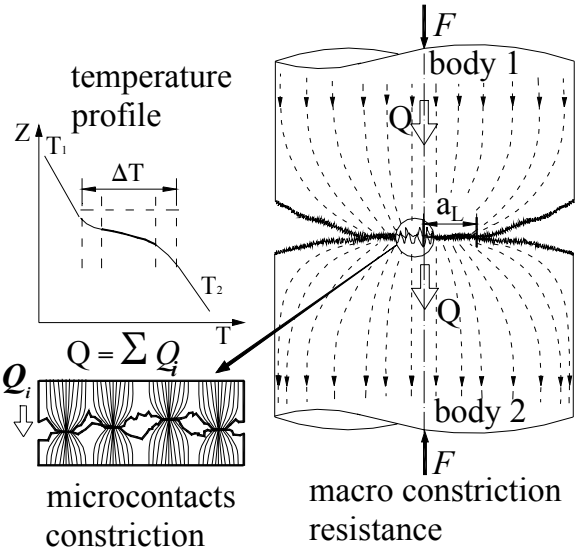

Fig. 1 Contact of two spherical rough surfaces in a vacuum

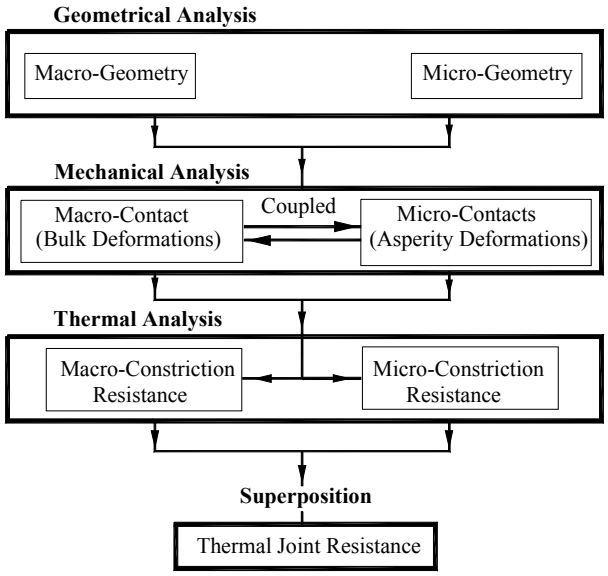

Fig. 2 Thermal contact problem

tronics cooling, spacecraft structures, satellite bolted joints, nuclear engineering, ball bearings, and heat exchangers. Due to roughness of the contacting surfaces, real contacts in the form of microcontacts occur only at the top of surface asperities, which are a small portion of the nominal contact area, normally less than 5 percent. As a result of curvature or out-of-flatness of the contacting bodies, a macrocontact area is formed, the area where the microcontacts are distributed.

Thermal energy can be transferred between contacting bodies by three different modes, i) conduction, through the microcontacts, ii) conduction, through the interstitial fluid in the gap between the solids, and iii) thermal radiation across the gap if the interstitial substance is transparent to radiation. According to Clausing and Chao[1] radiation heat transfer across the interface remains small as long as the body temperatures are not too high, i.e., less than 700 K, and in most typical applications can be neglected. In this study the surrounding environment is a vacuum, thus the only remaining heat transfer mode is conduction at the microcontacts. As illustrated in Fig. 1, heat flow is constrained to pass through the macrocontact, and then, in turn through the microcontacts. This phenomenon leads to a relatively high temperature drop across the interface.

Two sets of resistances in series can be used to represent the thermal contact resistance for a joint in a vacuum: the large-scale or macroscopic constriction resistance, R_L, and the small-scale or microscopic constriction resistance, R_s[1–3]

$$R_j = R_{mic} + R_{mac} \tag{1}$$

Many theoretical models for determining thermal contact resistance (TCR) have been developed for two limiting cases, i) conforming rough, where contacting surfaces are assumed to be perfectly flat, and ii) elastoconstriction, where the effect of roughness is neglected, i.e., contact of two smooth spherical surfaces. The above limiting cases are simplified cases of real contacts since engineering surfaces have both out-of-flatness and roughness simultaneously. As shown in Fig. 2, TCR problems basically consist of three separate problems: 1) geometrical, 2) mechanical, and 3) thermal, each sub-problem also includes a micro and macro scale component. The heart of TCR is the mechanical analysis. A mechanical model was developed and presented in the Part 1 of this study.[4] The mechanical analysis determines the macrocontact radius and the effective pressure distribution for the large-scale contact problem. While the microcontact analysis gives the local separation between the mean planes of the contacting bodies, the local mean size and the number of microcontacts. The results of the mechanical analysis are used in the thermal analysis to calculate the microscopic and macroscopic thermal constriction resistances.

A few analytical models for contact of two nonconforming rough surfaces exist in the literature. Bahrami et al.[5] reviewed existing analytical nonconforming rough TCR models and showed through comparison with experimental data that none of the existing models cover the above mentioned limiting cases and the transition region in which both roughness and out-of-flatness are present and their effects on TCR are of the same importance.

Theoretical Background

Thermal spreading resistance is defined as the difference between the average temperature of the contact area and the average temperature of the heat sink,

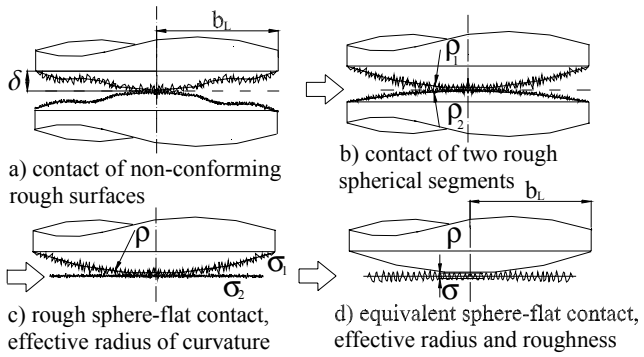

Fig. 3 Geometrical modeling

which is located far from the contact area, divided by the total heat flow rate Q,[6] $R = \Delta T/Q$. Thermal conductance is defined in the same manner as the film coefficient in convective heat transfer, $h = Q/(\Delta T A_a)$.

Considering the curvature or out-of-flatness of contacting surfaces in a comprehensive manner is very complex because of its random nature. Certain simplifications must be introduced to describe the macroscopic topography of surfaces using a few parameters. Theoretical approaches by Clausing and Chao,[1] Mikic and Rohsenow,[3] Yovanovich,[2] Nishino et al.,[7] and Lambert and Fletcher[8] assumed that a spherical profile might approximate the shape of the macroscopic nonuniformity. According to Lambert[9] this assumption is justifiable, because nominally flat engineering surfaces are often spherical, or crowned (convex) with a monotonic curvature in at least one direction. The relationship between the radius of curvature and the maximum out-of-flatness is[10]

$$\rho = \frac{b_L^2}{2\delta} \tag{2}$$

where δ is the maximum out-of-flatness of the surface.

As discussed in Bahrami et al.,[4] the contact between two Gaussian rough surfaces can be approximated by the contact between a single Gaussian surface, having the effective surface characteristics, placed in contact with a perfectly smooth surface. The contact of two spheres can be replaced by a flat in contact with a sphere incorporating an effective radius of curvature,[11] effective surface roughness and surface slope as given in Eq. (3)

$$\sigma = \sqrt{\sigma_1^2 + \sigma_2^2} \quad \text{and} \quad m = \sqrt{m_1^2 + m_2^2}$$
$$\frac{1}{\rho} = \frac{1}{\rho_1} + \frac{1}{\rho_2} \tag{3}$$

Figure 3 summarizes the geometrical procedure, which has been widely used for modeling the actual contact between non-conforming rough bodies.

When two non-conforming random rough surfaces are placed in mechanical contact, many microcontacts are formed within the macrocontact area. Microcontacts are small and located far from each other. Thermal contact models are constructed based on the premise that inside the macrocontact area a number of parallel cylindrical heat channels exist. The real shapes of microcontacts can be a wide variety of singly connected areas depending on the local profile of the contacting asperities. Yovanovich et al.[12] studied the steady state thermal constriction resistance of singly connected planar contacts of arbitrary shape. By using an integral formulation and a semi-numerical integration process applicable to any shape, they proposed a definition for thermal constriction resistance based on the square root of the contact area. A non-dimensional constriction resistance based on the square root of area was proposed, which varied by less than 5% for all shapes considered. Yovanovich et al.[12] concluded that the real shape of the contact was a second order effect, and an equivalent circular contact, where surface area is preserved, can be used to represent the contact.

As the basic element for macro and micro thermal analysis, thermal constriction of the flux tube was employed by many researchers. Figure 4 illustrates two flux tubes in a series contact. A flux tube consists of a circular heat sink or source, which is in perfect thermal contact with a long tube. Heat enters the tube from the source and leaves the tube at the other end. Cooper et al.[13] proposed a simple accurate correlation for calculating the thermal spreading resistance of the isothermal flux tube, (see Bahrami et al.[5] for more details):

$$R_{\text{flux tube 1}} + R_{\text{flux tube 2}} = \frac{\psi(\varepsilon)}{2k_s a} = \frac{(1-\varepsilon)^{1.5}}{2k_s a} \tag{4}$$

where $\varepsilon = a/b$, $k_s = 2k_1k_2/(k_1 + k_2)$, and $\psi(\cdot)$ is the spreading resistance factor. In Eq. (4), it is assumed that the radii of two contacting bodies are the same, i.e., $b_1 = b_2 = b$. In general case where $b_1 \neq b_2$, thermal spreading resistance will be, $R_{\text{flux tube}} = \psi(a/b)/4ka$.

Figure 5 illustrates the resistance network analogy for a thermal joint resistance analysis. The total joint resistance can be written as

$$R_j = R_{L,1} + R_{s,1} + R_{s,2} + R_{L,2} \tag{5}$$

where

$$\left(\frac{1}{R_s}\right)_{1,2} = \left(\sum_{i=1}^{n_s} \frac{1}{R_{s,i}}\right)_{1,2} \tag{6}$$

where n_s, $R_{s,i}$ are the number of microcontacts and the resistance of each microcontact, respectively. Subscripts 1, 2 signify bodies 1, 2.

The Present Model

In addition to the geometrical and mechanical assumptions, which were discussed in Bahrami et al.,[4] the remaining assumptions of the present model are:

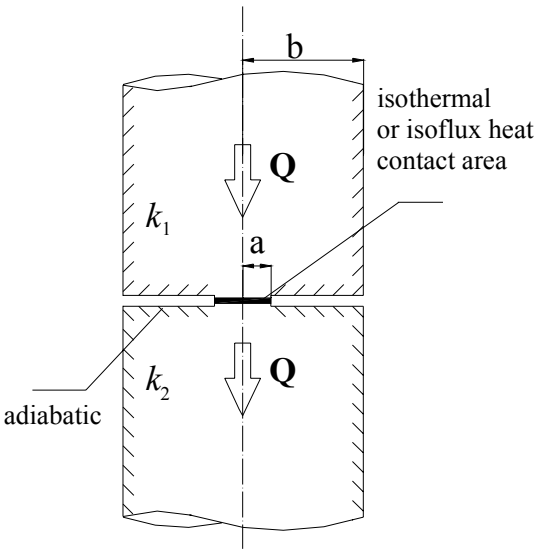

Fig. 4 Two flux tubes in series contact

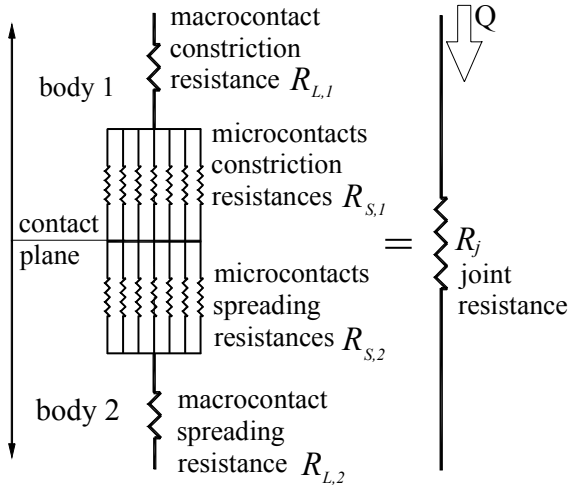

Fig. 5 Thermal resistance network for non-conforming rough contacts in a vacuum

- contacting solids are isotropic and thick relative to the roughness or waviness
- radiation heat transfer is negligible
- microcontacts are circular and steady-state heat transfer at microcontacts
- microcontacts are isothermal, Cooper et al.[13] proved that all microcontacts must be at the same temperature, provided the conductivity in each body is independent of direction, position and temperature.
- microcontacts are flat, it is justifiable since surface asperities have a very small slope[3]
- surfaces are clean and the contact is static

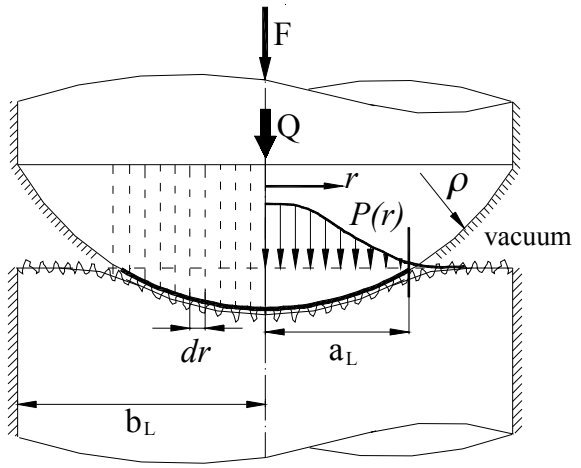

Fig. 6 Geometry of contact

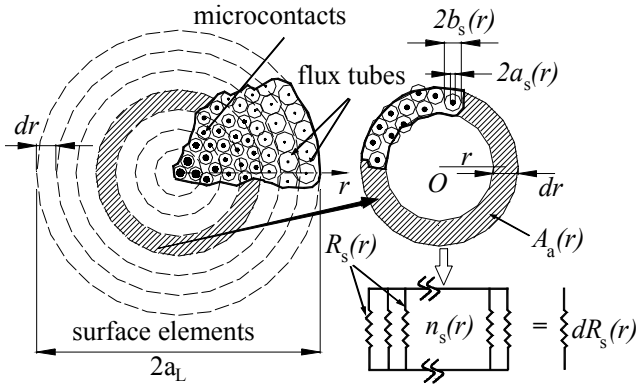

Fig. 7 Microcontacts distribution in contact area and thermal resistance network for a surface element

Figure 6 shows the geometry of the contact with equivalent radius of curvature and roughness where a_L is the radius of the macrocontact area and b_L is the radius of the contacting bodies.

The flux tube solution is employed to determine the macrocontact thermal resistance, i.e.,

$$R_L = \frac{(1 - a_L/b_L)^{3/2}}{2k_s a_L} \tag{7}$$

Separation between the mean planes of contacting bodies and pressure distribution are not uniform in the contact area, consequently, the number and the average size of microcontacts decrease as the radial position r increases. Figure 7 illustrates the modeled geometry of the microcontact distribution, macrocontact area the circle with radius a_L, is divided into surface elements, dashed rings with increment dr. Figure 7 illustrates the mean average size of microcontacts as small filled-circles. Around each microcontact a dashed circle illustrates the flux tube associated with

the microcontact. While microcontacts can vary in both size and shape, a circular contact of equivalent area can be used to approximate the actual microcontacts, since the local separation is uniform in each surface element.

Local spreading resistance for microcontacts can be calculated by applying the flux tube expression

$$R_s(r) = \frac{\psi[\varepsilon(r)]}{2k_s a_s(r)} \tag{8}$$

where $\varepsilon(r) = a_s(r)/b_s(r)$ is the local microcontacts relative radius, $a_s(r)$, $\psi(\cdot)$ are the local mean average microcontact radius and the spreading resistance factor given by Eq. (4).

Local microcontact relative radius and microcontact local density can be calculated from[4]

$$\varepsilon(r) = \sqrt{\frac{A_r(r)}{A_a(r)}} = \sqrt{\frac{1}{2}\text{erfc }\lambda(r)} \tag{9}$$

$$n_s = \frac{1}{16}\left(\frac{m}{\sigma}\right)^2 \frac{\exp\left[-2\lambda(r)^2\right]}{\text{erfc }\lambda(r)} A_a \tag{10}$$

where $\lambda(r) = Y(r)/\sqrt{2}\sigma$, A_r and A_a are nondimensional separation, and real and apparent contact area, respectively.

The thermal resistance network for the surface elements is shown in Fig. 7. In each element $n_s(r)$ microcontacts exist which provide identical parallel paths for transferring thermal energy. Therefore, microcontact thermal resistance for a surface element $dR_s(r)$ is

$$dR_s(r) = \frac{R_s(r)}{n_s(r)} \tag{11}$$

As shown in Fig. 8, surface elements form another set of parallel paths for transferring thermal energy in the macrocontact area. Therefore, the effective micro thermal resistance for the joint is

$$R_s = \frac{1}{\sum 1/dR_s(r)} \tag{12}$$

The joint resistance is the sum of the macro and micro thermal resistances, i.e., $R_j = R_L + R_s$.

Results

As explained in Bahrami et al.,[4] a simulation routine was developed to calculate the thermal joint resistance. As an example, contact of a 25 (mm) sphere with a flat was considered and solved with the routine. The contacting bodies are stainless steel and Table 1 lists the surfaces parameters. The mechanical results were presented in Bahrami et al.[4] and Figs. 9 and 10 present thermal outputs. As expected, the thermal resistance of the microcontacts (resistance of the local mean microcontact) increases as r increases. The microcontact relative radius ε has its maximum value at the center

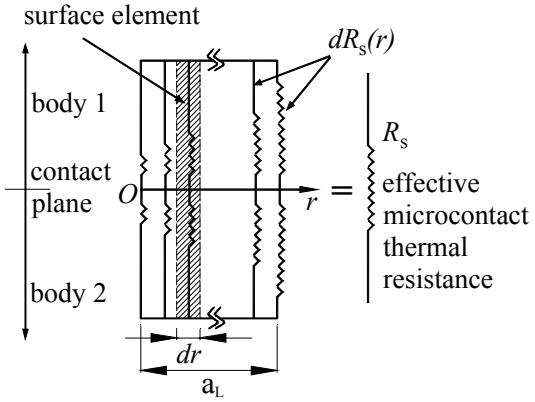

Fig. 8 Thermal resistance network for surface elements

Table 1 Input parameters for a typical contact problem

$\rho = 25\,(mm)$	$F = 50\,(N)$
$\sigma = 1.41\,(\mu m)$	$E' = 112.1\,(GPa)$
$m = 0.107\,(-)$	$c_1/c_2 = 6.27\,(GPa)\,/\,-0.15\,(-)$
$b_L = 25\,(mm)$	$k_s = 16\,(W/mK)$

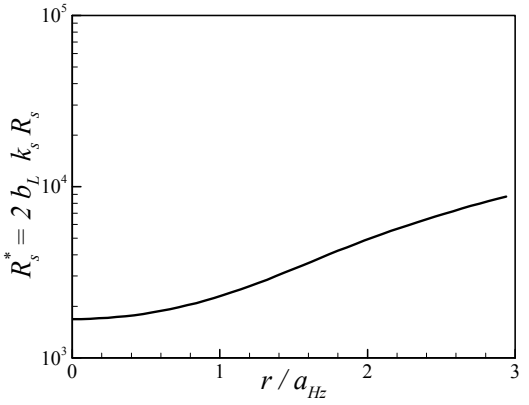

Fig. 9 Micro thermal contact resistance

of the contact and decreases with increasing radial position r.

To investigate the effect of input parameters on thermal joint resistance, the program was run for a range of each input parameter, while the remaining parameters in Table 1 were held constant. Additionally, elastoconstriction thermal resistance introduced by Yovanovich[14] indicated by R_{Hz}, was also included in the study. Elastoconstriction is a limiting case in which the surfaces are assumed to be perfectly smooth, i.e., $a_L = a_{Hz}$ and $R_s = 0$.

The effect of roughness on macro, micro, and joint resistances are shown in Fig. 11. Recall that the joint resistance is the summation of the macro and micro contact resistances. With relatively small roughness,

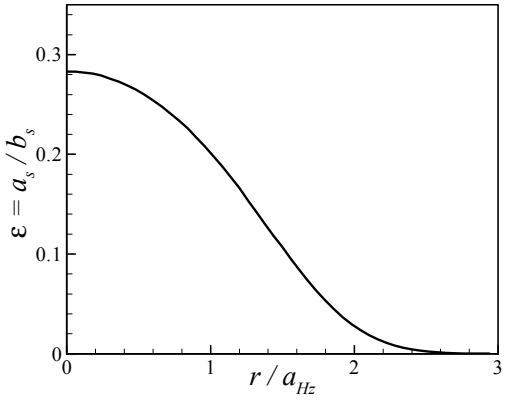

Fig. 10 Microcontact relative radius

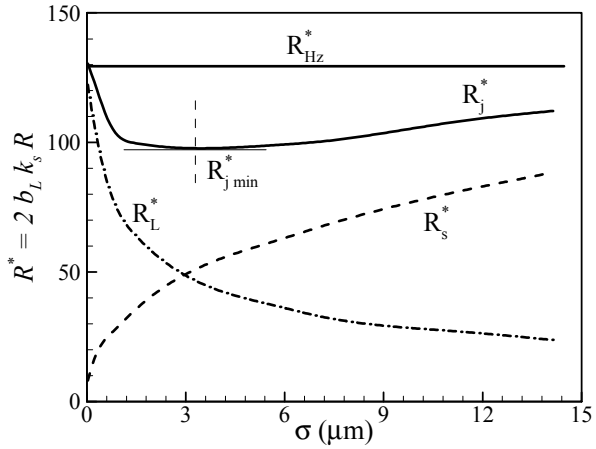

Fig. 11 Effect of roughness on TCR

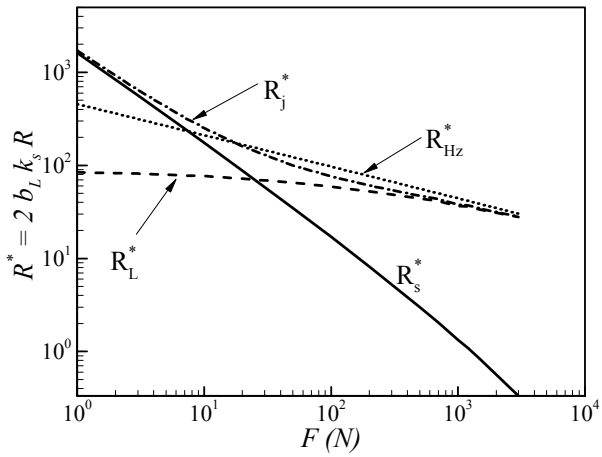

Fig. 12 Effect of load on TCR

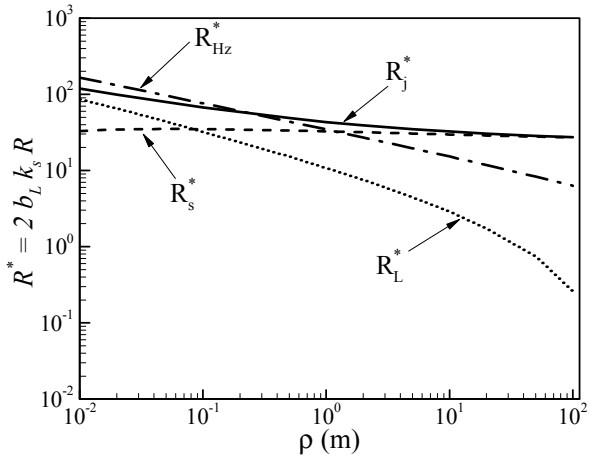

Fig. 13 Effect of radius of curvature on TCR

the macro thermal resistance dominates the joint resistance and the micro thermal resistance is negligible, also the joint resistance is close to the elastoconstriction thermal resistance. By increasing roughness, a_L becomes larger thus, the macro thermal resistance decreases, while the micro thermal resistance increases, at some point they become comparable in size, by further increase in the roughness micro thermal resistance controls the joint resistance. It also can be seen from Fig. 11 that for a fixed geometry and load, there is a roughness that minimizes the thermal joint resistance.

The effect of load on micro, macro and joint thermal resistance is shown in Fig. 12. At light loads, due to the small number and size of the microcontacts, the micro thermal resistance dominates. As the load increases the joint resistance decreases continuously, micro and macro thermal resistances become comparable in size and at larger loads the macro thermal resistance becomes the controlling part. At higher loads the joint resistance approaches the elastoconstriction resistance as if no roughness exists. Figure 13 shows the effect of radius of curvature. At very small radii, the macro thermal resistance dominates due to the small size of macrocontacts. As the radius of curvature increases, approaching flat surface, the micro thermal resistance becomes more important and the macro resistance becomes smaller and eventually when $a_L = b_L$ the macro resistance falls to zero.

Alternative Approach

The goal of this study is to develop simple correlations for determining TCR. In this section, a general expression for the micro thermal spreading resistance is derived, which in conjunction with the macro thermal resistance, Eq. (7), gives a correlation to calculate the thermal joint resistance in a vacuum environment.

The amount of heat transferred in a non-conforming rough contact is

$$Q = \sum dQ = \iint_{contact\ plane} dQ \qquad (13)$$

where dQ is the heat transferred in a surface element.

The local thermal joint conductance is a function of r

$$Q = \iint_{contact\ plane} h_s(r)\,\Delta T_s dA_a \tag{14}$$

where dA_a and ΔT_s = constant are the area of a surface element and the temperature drop, respectively. Since the macrocontact area is approximated as a circle

$$Q = 2\pi\Delta T_s \int_0^{a_L} h_s(r)\, r dr \tag{15}$$

The effective thermal micro-conductance for a joint is defined as: $h_s = Q/A_a\Delta T_s$. Therefore, the effective microcontact conductance can be found from

$$h_s = \frac{2\pi}{A_a}\int_0^{a_L} h_s(r)\, r dr \tag{16}$$

or in terms of thermal resistance where $R = 1/(hA_a)$,

$$R_s = \frac{1}{2\pi\int_0^{a_L} h_s(r)\, r dr} \tag{17}$$

Yovanovich[15] suggested an expression for thermal conductance of conforming rough contacts as

$$h_s = 1.25 k_s \left(\frac{m}{\sigma}\right)\left(\frac{P}{H_{mic}}\right)^{0.95} \tag{18}$$

where H_{mic} and m are the microhardness of the softer material in contact and the mean absolute slope of asperities, respectively. Combining Eqs. (17) and (18), a relationship between thermal micro-resistance and pressure distribution can be found as

$$R_s = \frac{\sigma}{2.5\pi m k_s}\left[\int_0^{a_L}\left[\frac{P(r)}{H_{mic}(r)}\right]^{0.95} r dr\right]^{-1} \tag{19}$$

Microhardness depends on several parameters: mean surface roughness σ, mean absolute slope of asperities, m, type of material, method of surface preparation, and applied pressure. According to Hegazy,[16] surface microhardness can be introduced into the calculation of relative contact pressure in the form of the Vickers microhardness

$$H_v = c_1 (d_v')^{c_2} \tag{20}$$

where H_v is the Vickers microhardness in (GPa), $d_v' = d_v/d_0$ and $d_0 = 1\,(\mu m)$, d_v is the Vickers indentation diagonal in μm and c_1 and c_2 are correlation coefficients determined from Vickers microhardness measurements. Song and Yovanovich[17] developed an explicit expression relating microhardness to the applied pressure

$$\frac{P}{H_{mic}} = \left(\frac{P}{H'}\right)^{\frac{1}{1+0.071c_2}} \tag{21}$$

where $H' = c_1(1.62\sigma'/m)^{c_2}$, $\sigma' = \sigma/\sigma_0$ and $\sigma_0 = 1\ \mu m$.

Sridhar and Yovanovich[18] developed empirical relations to estimate the Vickers microhardness coefficients, using the bulk hardness of the material. Two least-square-cubic fit expressions were reported:

$$c_1 = H_{BGM}\left(4.0 - 5.77\kappa + 4.0\kappa^2 - 0.61\kappa^3\right) \tag{22}$$

$$c_2 = -0.57 + \frac{1}{1.22}\kappa - \frac{1}{2.42}\kappa^2 + \frac{1}{16.58}\kappa^3 \tag{23}$$

where $\kappa = H_B/H_{BGM}$, H_B is the Brinell hardness of the bulk material, and $H_{BGM} = 3.178\ GPa$. The above correlations are valid for the range $1.3 \le H_B \le 7.6\ GPa$ with the RMS percent difference between data and calculated values were reported; 5.3% and 20.8% for c_1, and c_2, respectively. However, in situations where an effective value for microhardness $H_{mic,e}$ is known the microhardness coefficients can be calculated from $c_1 = H_{mic,e}$ and $c_2 = 0$.

Combining Eqs.(19), and (21) gives

$$R_s = \frac{\sigma H'^s}{2.5\pi k_s m\int_0^{a_L}[P(r)]^s\, r dr} \tag{24}$$

where $s = 0.95/(1 + 0.071c_2)$. Bahrami et al.[4] proposed expressions for the pressure distribution of spherical rough contacts which covers all possible contact cases including flat contacts

$$P(\xi) = \begin{cases} F/\pi b_L^2 & F_c = 0 \\ P_0\left(1-\xi^2\right)^{\gamma} & F \le F_c \\ P_{0,c}\left(1-\xi^2\right)^{\gamma_c} + \dfrac{F-F_c}{\pi b_L^2} & F \ge F_c \end{cases} \tag{25}$$

where $\xi = r/a_L$, $\gamma = 1.5\,(P_0/P_{0,Hz})\,(a_L/a_{Hz})^2 - 1$. F_c is the critical force where $a_L = b_L$ and it is given by

$$F_c = \frac{4E'}{3\rho}\left[\max\left\{0, \left(b_L^2 - 2.25\sigma\rho\right)\right\}\right]^{3/2} \tag{26}$$

where $\max\{x, y\}$ returns the maximum value between x and y. A criterion for defining the flat surface was derived.[4] It was shown that if the out-of-flatness/waviness and the roughness of a surface are of the same order of magnitude, the surface is flat, i.e., $\delta/\sigma \le 1.12$.

Substituting the pressure distribution, for $F \le F_c$ into Eq. (24) one can obtain

$$R_s = \frac{\sigma\,(H'/P_0)^s}{2.5\pi\ m\ k_s\ a_L^2}\left[\int_0^1 \left(1-\xi^2\right)^{s\gamma}\,\xi\ d\xi\right]^{-1} \tag{27}$$

Evaluating the integral, one can obtain

$$R_s = \frac{\sigma\,(1+s\gamma)}{1.25\pi\ m\ k_s\ a_L^2}\left(\frac{H'}{P_0}\right)^s \tag{28}$$

For $F \ge F_c$, the effective microcontact thermal resistance, after evaluating the integral, becomes

$$R_s = \frac{\sigma}{1.25\pi m k_s\ b_L^2}\left[\left(\frac{H'}{P_{0,c}}\right)^s(1+s\gamma_c) + \left(\frac{\pi H' b_L^2}{F-F_c}\right)^s\right] \tag{29}$$

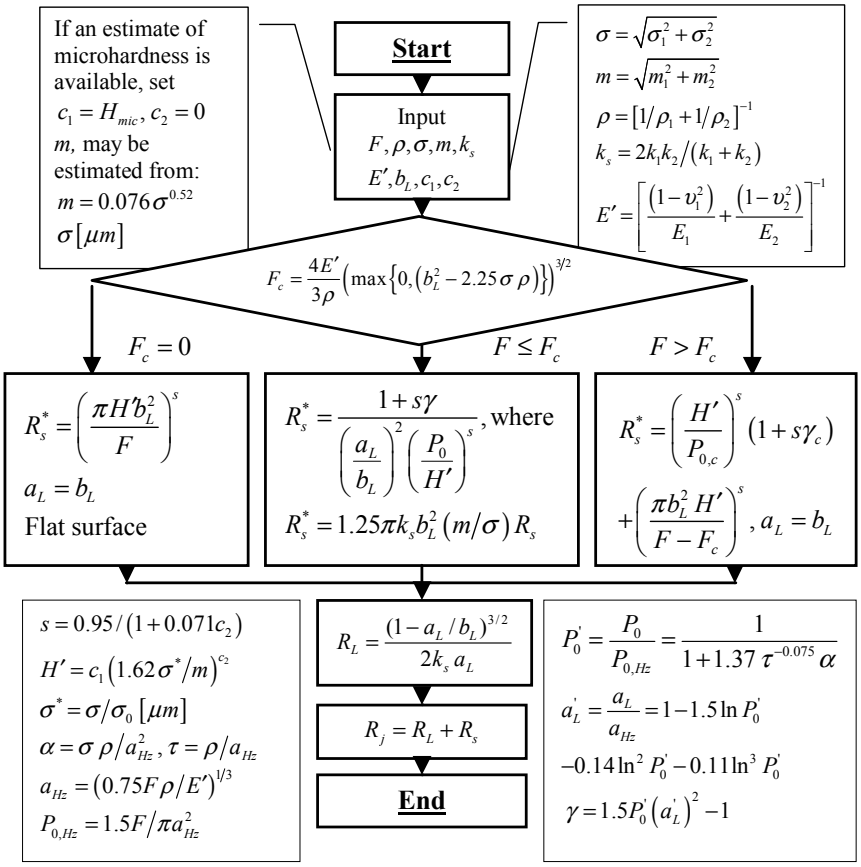

Fig. 14 Procedure for utilizing the present model

Table 2 Range of parameters for the experimental data

Parameter
$7.15 \le b_L \le 14.28\,(mm)$
$25.64 \le E' \le 114.0\ (GPa)$
$7.72 \le F \le 16763.9\,(N)$
$16.6 \le k_s \le 227.2\ (W/mK)$
$0.04 \le m \le 0.34\ (-)$
$0.12 \le \sigma \le 13.94\ (\mu m)$
$0.013 \le \rho \lessapprox 120\ (m)$

where $P_{0,c}$ and γ_c are the values at the critical force. The general relationship for micro thermal resistance can be summarized as

$$R_s^* = \begin{cases} \left(\dfrac{\pi H' b_L^2}{F}\right)^s & F_c = 0 \\ \left(\dfrac{b_L}{a_L}\right)^2 \left(\dfrac{H'}{P_0}\right)^s (1+s\gamma) & F \le F_c \\ \left(\dfrac{H'}{P_{0,c}}\right)^s (1+s\gamma_c) + \left(\dfrac{\pi H' b_L^2}{F - F_c}\right)^s & F \ge F_c \end{cases} \tag{30}$$

Table 3 Reseacher and specimen materials used in comparisons

Ref.	Researcher	Material(s)
A	Antonetti[19]	Ni200 Ni200-Ag
B	Burde[20]	SPS 245, CS
CC	Clausing-Chao[1]	Al2024 T4 Brass Anaconda Mg AZ 31B SS303
F	Fisher[21]	Ni 200-Carbon Steel
H	Hegazy[16]	Ni200 SS304 Zircaloy4 Zr-2.5%wt Nb
K	Kitscha[22]	Steel 1020-CS
MM	McMillan-Mikic[23]	SS303
MR	Mikic-Rohsenow[3]	SS305
M	Milanez et al.[24]	SS304

where $R_s^* = 1.25\pi b_L^2 k_s (m/\sigma) R_s$. Figure 14 summarizes the procedure used to implement the present model.

Comparison With Experimental Data

During the last four decades a large number of experimental data have been collected for a wide variety

of materials such as brass, magnesium, nickel 200, silver and stainless steel in a vacuum. More than 700 data points were collected from an extensive review of the literature, summarized and compared with the present model. As summarized in Table 2, the experimental data form a complete set of the materials with a wide range of mechanical, thermal, and surfaces characteristics used in applications where TCR is of concern. The data also include the contact between dissimilar metals such as Ni200-Ag and SS-CS.

Generally, TCR experimental procedures include two cylindrical specimens with the same diameter b_L which are pressed coaxially together by applying an external load in a vacuum chamber. After reaching steady state conditions, TCR is measured at each load. These experiments have been conducted by many researchers including Burde[20] and Clausing and Chao.[1] Table 3 indicates the researchers, reference publications, specimen designation, and the material type used in the experiments.

The comparison includes all three regions of TCR, i.e., the conforming rough, the elastoconstriction and the transition. Tables 4 and 5 list the experiment number, i.e., the number which was originally assigned to a particular experimental data set by the researchers and geometrical, mechanical and thermal properties of the experimental data, as reported. Clausing and Chao,[1] Fisher,[21] Kitscha,[22] and Mikic and Rohsenow[3] did not report the surface slope m; however the Lambert[9] correlation was used to estimate these values (see Fig. 14). Additionally, the exact values of radii of curvature for conforming rough surfaces were not reported. Since, these surfaces were prepared to be optically flat, radii of curvature in the order of $\rho \approx 100\,(m)$ are considered for these surfaces.

Figure 15 illustrates the comparison between the present model and the experimental data, with

$$R_j^* = k_s b_L R_j$$
$$\Omega = \frac{(\sigma/m)\,(1+s\gamma)}{1.25\pi b_L B^2}\left(\frac{H'}{P_0}\right)^s + \frac{(1-B)^{1.5}}{2B} \quad (31)$$

where $B = a_L/b_L \leq 1$ and R_j^* is the non-dimensional thermal joint resistance. From Eqs. (7), (30), and (31) it can be seen that the parameter Ω is the non-dimensional TCR predicted by the model, i.e., $\Omega = R_s^* + R_j^*$ or $R_j^* = \Omega$. Therefore the model is shown by the 45-degree line in Fig. (15). The procedure to implement the model and all required relationships are summarized in Fig. 14; equivalently, TCR can be determined using Eq. (31). Bahrami et al.[4] proposed the following expression for calculating a'_L

$$a'_L = \frac{a_L}{a_{Hz}} = \frac{1.80\sqrt{\alpha + 0.31\ \tau^{0.056}}}{\tau^{0.028}} \quad (32)$$

Using Eq. (32) one can find a relationship for B as a function of non-dimensional and geometrical parameters, i.e.,

$$B = \frac{a_L}{b_L} = 1.80\left(\frac{a_{Hz}}{b_L}\right)\frac{\sqrt{\alpha + 0.31\ \tau^{0.056}}}{\tau^{0.028}} \quad (33)$$

Table 4 Summary of geometrical, mechanical and thermophysical properties, rough sphere-flat contacts

Ref.	E'	σ/m	ρ	$c_1/-c_2$	k_s	b_L
B,A-1	114.0	0.63/.04	.013	3.9/0	40.7	7.2
B,A-2	114.0	1.31/.07	.014	3.9/0	40.7	7.2
B,A-3	114.0	2.44/.22	.014	3.9/0	40.7	7.2
B,A-4	114.0	2.56/.08	.019	4.4/0	40.7	7.2
B,A-5	114.0	2.59/.10	.025	4.4/0	40.7	7.2
B,A-6	114.0	2.58/.10	.038	4.4/0	40.7	7.2
CC,2A	38.66	0.42/-	14.0	1.6/.04	141	12.7
CC,8A	38.66	2.26/-	14.7	1.6/.04	141	12.7
CC,1B	49.62	0.47/-	3.87	3.0/.17	125	12.7
CC,2B	49.62	0.51/-	4.07	3.0/.17	125	12.7
CC,3B	49.62	0.51/-	3.34	3.0/.17	102	12.7
CC,4B	49.62	0.51/-	4.07	3.0/.17	125	12.7
CC,3S	113.7	0.11/-	21.2	4.6/.13	17.8	12.7
CC,2M	25.64	0.11/-	30.3	.41/0	96	12.7
F,11A	113.1	0.12/-	.019	4.0/0	57.9	12.5
F,11B	113.1	0.12/-	.038	4.0/0	57.9	12.5
F,13A	113.1	0.06/-	.038	4.0/0	58.1	12.5
K,T1	113.8	0.76/-	.014	4.0/0	51.4	12.7
K,T2	113.8	0.13/-	.014	4.0/0	51.4	12.7
MM,T1	113.7	2.7/.06	.128	4.0/0	17.3	12.7
MM,T2	113.7	1.75/.07	2.44	4.0/0	22	12.7
MR,T1	107.1	4.83/-	21.2	4.2/0	19.9	12.7
MR,T2	107.1	3.87/-	39.7	4.2/0	19.9	12.7

Experimental data are distributed over four decades of Ω from approximately 0.03 up to 70. The model shows good agreement with the data over the entire range of comparison with the exception of a few points.

In most of the conforming rough data sets, such as Hegazy,[16] experimental data show a lower resistance at relatively light loads in comparison with the model and the data approach the model as the load increases. This trend can be observed in almost all conforming rough data sets (see Fig. 15). This phenomenon which is called the *truncation effect*[24] is important at light loads when surfaces are relatively rough. A possible reason for this behavior is the Gaussian assumption of the surface asperities which implies that asperities with "infinite" heights exist. Milanez et al.[24] experimentally studied the truncation effect and proposed correlations for maximum asperities heights as functions of surface roughness.

Because of the above-mentioned approximations to account for unreported data, the accuracy of the model is difficult to assess. However, the RMS and the average absolute difference between the model and data for the entire set of data are approximately 11.4% and 10.0%, respectively.

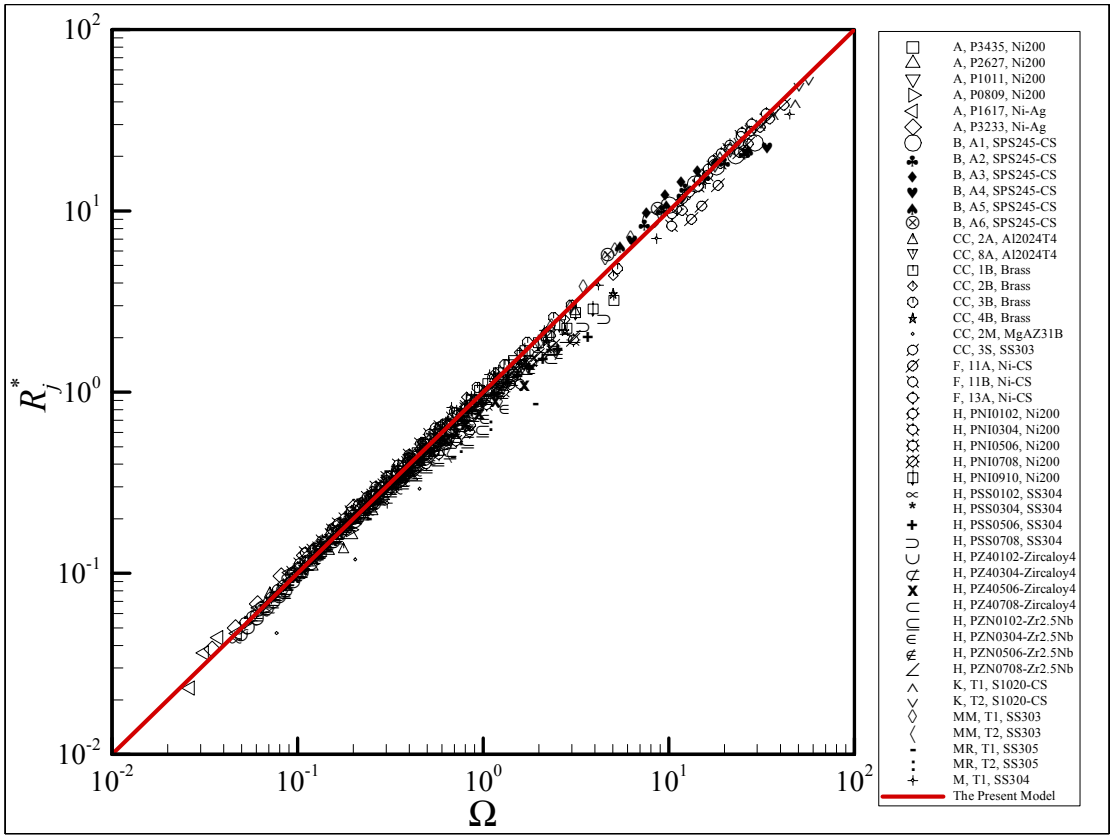

Fig. 15 Comparison of present model with experimental data

Table 5 Summary of geometrical, mechanical and thermophysical properties for conforming rough contacts

Ref.	E'	σ	m	c_1	-c_2	k_s	b_L
A,P3435	112.1	8.48	.34	6.3	.26	67.1	14.3
A,P2627	112.1	1.23	.14	6.3	.26	64.5	14.3
A,P1011	112.1	4.27	.24	6.3	.26	67.7	14.3
A,P0809	112.1	4.29	.24	6.3	.26	67.2	14.3
A,P1617	63.9	4.46	.25	.39	0	100	14.3
A,P3233	63.9	8.03	.35	.39	0	100	14.3
H,NI12	112.1	3.43	.11	6.3	.26	75.3	12.5
H,NI34	112.1	4.24	.19	6.3	.26	76.0	12.5
H,NI56	112.1	9.53	.19	6.3	.26	75.9	12.5
H,NI78	112.1	13.9	.23	6.3	.26	75.7	12.5
H,NI910	112.1	0.48	.23	6.3	.26	75.8	12.5
H,SS12	112.1	2.71	.07	6.3	.23	19.2	12.5
H,SS34	112.1	5.88	.12	6.3	.23	19.1	12.5
H,SS56	112.1	10.9	.15	6.3	.23	18.9	12.5
H,SS78	112.1	0.61	.19	6.3	.23	18.9	12.5
H,Z412	57.3	2.75	.05	3.3	.15	16.6	12.5
H,Z434	57.3	3.14	.15	3.3	.15	17.5	12.5
H,Z456	57.3	7.92	.13	3.3	.15	18.6	12.5
H,Z478	57.3	0.92	.21	3.3	.15	18.6	12.5
H,ZN12	57.3	2.50	.08	5.9	.27	21.3	12.5
H,ZN34	57.3	5.99	.16	5.9	.27	21.2	12.5
H,ZN56	57.3	5.99	.18	5.9	.27	21.2	12.5
H,ZN78	57.3	8.81	.20	5.9	.27	21.2	12.5
M,SS1	113.8	0.72	.04	6.3	.23	18.8	12.5

Concluding Remarks

TCR of non-conforming rough surfaces was considered as the superposition of macro and micro thermal resistance components accounting for the effects of surface curvature and roughness, respectively. TCR were categorized into three main regions, 1) the conforming rough limit; where the contacting surfaces are flat and the effect of surface curvature can be ignored; thus the micro thermal resistance dominates the joint resistance, 2) the elastoconstriction limit in which the radii of the contacting bodies are relatively small and the effect of roughness on the TCR is negligible and the macro resistance is the controlling part, and 3) the transition region where the macro and micro thermal resistances are comparable.

The results of the mechanical model presented in Bahrami et al.,[4] i.e., the local mean separation, the local mean radius and the number of microcontacts, were used to develop an analytical thermal model for determining TCR of non-conforming rough contacts in a vacuum. The thermal model was constructed based on the premise that the mean separation between the contacting surfaces in an infinitesimal surface element can be assumed constant. Therefore, the conforming rough model of Cooper et al.[13] could be implemented to calculate the surface element thermal resistance. The surface element thermal resistances were integrated over the macrocontact area to calculate the effective

micro thermal resistance of the contact. The macro-contact resistance was calculated using the flux tube solution.

The effects of the major parameters, i.e., roughness, load, and radius of curvature on TCR were investigated. It was shown that there is a value of surface roughness that minimizes TCR. Additionally, at large loads the effect of roughness on the TCR becomes negligible.

By using the general pressure distribution introduced in Bahrami et al.[4] and the Yovanovich[15] correlation for thermal conductance of conforming rough contacts, simple correlations for determining TCR were derived which cover the entire range of TCR from conforming rough to smooth spherical contacts. The procedure for implementing the present model was presented in the form of a simple algorithm. The input parameters to utilize the proposed correlations are: load F, the effective elasticity modulus E', Vickers microhardness correlation coefficients c_1 and c_2, effective surface roughness σ and surface slope m, the effective surface out-of-flatness δ or radius of curvature ρ, radius of the contacting surfaces b_L, and the harmonic mean of the thermal conductivities k_s.

The present model was compared with more than 700 experimental data points and showed good agreement over the entire range of TCR. The RMS difference between the model and the data was estimated to be approximately 11.4%. The list of materials in the comparison formed a complete set of the metals used in applications, where TCR is of concern. It was also shown that the present model is applicable to dissimilar metals.

References

[1]Clausing, A. M. and Chao, B. T., "Thermal Contact Resistance in a Vacuum Environment," Tech. rep., University of Illinois, Urbana, Illinois, Report ME-TN-242-1, August, 1963.

[2]Yovanovich, M. M., "Overall Constriction Resistance Between Contacting Rough, Wavy Surfaces," *International Journal of Heat and Mass Transfer*, Vol. 12, 1969, pp. 1517–1520.

[3]Mikic, B. B. and Rohsenow, W. M., "Thermal Contact Conductance," Tech. rep., Dept. of Mech. Eng. MIT, Cambridge, Massachusetts, NASA Contract No. NGR 22-009-065, September, 1966.

[4]Bahrami, M., Culham, J. R., Yovanovich, M. M., and Schneider, G. E., "Thermal Contact Resistance of Non-Conforming Rough Surfaces Part 1: Mechanical Model," *AIAA Paper No. 2003-4197, 36th. AIAA Thermophysics Conference, June 23-26, Orlando, Florida*, 2003.

[5]Bahrami, M., Culham, J. R., Yovanovich, M. M., and Schneider, G. E., "Review Of Thermal Joint Resistance Models For Non-Conforming Rough Surfaces In A Vacuum," *Paper No. HT2003-47051, ASME Heat Transfer Conference, July 21-23, Rio Hotel, Las Vegas, Nevada*, 2003.

[6]Carslaw, H. S. and Jaeger, J. C., *Conduction of Heat in Solids, 2nd. Edition*, Oxford University Press, London, UK, 1959.

[7]Nishino, K., Yamashita, S., and Torii, K., "Thermal Contact Conductance Under Low Applied Load in a Vacuum Environment," *Experimental Thermal and Fluid Science, Elsevier*, Vol. 10, 1995, pp. 258–271.

[8]Lambert, M. A. and Fletcher, L. S., "Thermal Contact Conductance of Spherical Rough Metals," *Transactions of ASME, November*, Vol. 119, 1997, pp. 684–690.

[9]Lambert, M. A., *Thermal Contact Conductance of Spherical Rough Metals*, Ph.D. thesis, Texas A & M University, Dept. of Mech. Eng.,Texas, USA, 1995.

[10]Clausing, A. M. and Chao, B. T., "Thermal Contact Resistance in a Vacuum Environment," *Paper No.64-HT-16, Transactions of ASME: Journal of Heat Transfer*, Vol. 87, 1965, pp. 243–251.

[11]Hertz, H., "On the Contact of Elastic Bodies," *Journal fur die reine und angewandie Mathematic, (in German)*, Vol. 92, 1881, pp. 156–171.

[12]Yovanovich, M. M., Burde, S. S., and Thompson, C. C., "Thermal Constriction Resistance of Arbitrary Planar Contacts With Constant Flux," *AIAA 11th Thermophysics Conference, San Diego, California, July 14-16, Paper No. 76-440*, 1969, pp. 127–139.

[13]Cooper, M. G., Mikic, B. B., and Yovanovich, M. M., "Thermal Contact Conductance," *International Journal of Heat and Mass Transfer*, Vol. 12, 1969, pp. 279–300.

[14]Yovanovich, M. M., "Recent Developments In Thermal Contact, Gap and Joint Conductance Theories and Experiment," *Eighth International Heat Transfer Conference, San Francisco, CA, August 17- 22*, 1986, pp. 35–45.

[15]Yovanovich, M. M., "Thermal Contact Correlations," *Progress in Aeronautics and Aerodynamics: Spacecraft Radiative Transfer and Temperature Control, in Horton, T.E. (editor)*, Vol. 83, 1982, pp. 83–95.

[16]Hegazy, A. A., *Thermal Joint Conductance of Conforming Rough Surfaces: Effect of Surface Micro-Hardness Variation*, Ph.D. thesis, University of Waterloo, Dept. of Mech. Eng., Waterloo, Canada, 1985.

[17]Song, S. and Yovanovich, M. M., "Relative Contact Pressure: Dependence on Surface Roughness and Vickers Microhardness," *AIAA Journal of Thermophysics and Heat Transfer*, Vol. 2, No. 1, 1988, pp. 43–47.

[18]Sridhar, M. R. and Yovanovich, M., "Empirical Methods to Predict Vickers Microhardness," *WEAR*, Vol. 193, 1996, pp. 91–98.

[19]Antonetti, V. W., *On the Use of Metallic Coatings to Enhance Thermal Conductance*, Ph.D. thesis, University of Waterloo, Dept. of Mech. Eng., Waterloo, Canada, 1983.

[20]Burde, S. S., *Thermal Contact Resistance Between Smooth Spheres and Rough Flats*, Ph.D. thesis, University of Waterloo, Dept. of Mech. Eng., Waterloo, Canada, 1977.

[21]Fisher, N. F., *Thermal Constriction Resistance of Sphere/Layered Flat Contacts: Theory and Experiment*, Master's thesis, University of Waterloo, Dept. of Mech. Eng., Waterloo, Canada, 1987.

[22]Kitscha, W., *Thermal Resistance of the Sphere-Flat Contact*, Master's thesis, University of Waterloo, Dept. of Mech. Eng., Waterloo, Canada, 1982.

[23]McMillan, R. and Mikic, B. B., "Thermal Contact Resistance With Non-Uniform Interface Pressures," Tech. rep., Dept. of Mech. Eng. MIT, Cambridge, Massachusetts, NASA Contract No. NGR 22-009-(477), November, 1970.

[24]Milanez, F. H., Yovanovich, M. M., and Mantelli, M. B. H., "Thermal Contact Conductance at Low Contact Pressures," *AIAA Paper No. 2003-3489, 36th. AIAA Thermophysics Conference, June 23-26, Orlando, Florida*, 2003.